BOREAS An international journal of Quaternary research

Limnological response to the Laacher See eruption (LSE) in an annually laminated Allerød sediment sequence from the Nahe palaeolake, northern Germany

STEFAN DREIBRODT, SASCHA KRÜGER, JAN WEBER AND INGO FEESER

BOREAS

Dreibrodt, S., Krüger, S., Weber, J. & Feeser, I.: Limnological response to the Laacher See eruption (LSE) in an annually laminated Allerød sediment sequence from the Nahe palaeolake, northern Germany. *Boreas*. https://doi.org/10.1111/bor.12468. ISSN 0300-9483.

This paper presents evidence for a limnological response to the Laacher See eruption (LSE) as detected in lake sediments from Nahe, northern Germany. The sediment section of the Allerød period dating to between 13 422 and 12 708 cal. a BP is preserved in annual laminations. Within this section, the LSE was identified as a cryptotephra layer (12 944±44 cal. a BP). Microfacies analysis, continuous high-resolution geochemical measurements and pollen analyses enabled a high-resolution reconstruction of environmental change. The older part of the Allerød (*c.* 13 422 to 12 943 cal. a BP) was characterized by relatively stable sedimentation conditions. Evidence for windier conditions dating to *c.* 13 160 to 13 080 cal. a BP probably reflects the Gerzensee oscillation. Pronounced changes of the lake sedimentation followed the LSE. Four unusually thick varves with increased amounts of allochthonous material indicate serious disturbance of the local environment immediately after the LSE, related to increased storminess and/or the occurrence of high intensity rainfall events. A pronounced reduction of biogenic silica accumulation for *c.* 60 years after the LSE could reflect a period of acidification. Indications of a simultaneous lake level increase until *c.* 60 years after the LSE are in line with the supposed reduced evapotranspiration associated with cooler conditions. About 120 years after the LSE, increased oxygen access at the lake bottom, allochthonous input and Cl fluxes point to an onset of increasingly stronger westerly winds, probably as a long-term response to the LSE. This supports the idea of a southward shift of the mid-latitude westerlies wind system within the interval between the LSE and the beginning of the Younger Dryas. The pace of the southwards shift of this wind system decreased from 10 km a^{-1} in the initial phase (40–120 years after LSE) to 6 km a^{-1} in the later phase (120–200 years after LSE).

Stefan Dreibrodt (sdreibrodt@ecology.uni-kiel.de), Institute for Ecosystem Research, Kiel University, Olshausenstrasse 40, Kiel D - 24098, Germany; Sascha Krüger, Centre for Baltic and Scandinavian Archaeology (ZBSA), Schloss Gottorf, Schleswig D - 24837, Germany; Jan Weber, Institute of Geosciences, Kiel University, Ludewig-Meyn-Straße 10, Kiel D - 24118, Germany; Ingo Feeser, Institute of Pre- and Protohistoric Archaeology, Kiel University, Johanna-Mestorf-Straße 2-6, Kiel D - 24118, Germany; *received 16th January 2020, accepted 1st July 2020.*

The consequences of the Laacher See eruption (LSE) for central European environments and groups of humans have been discussed for more than three decades by palaeoenvironmentalists (e.g. Merkt 1971; Lotter & Birks 1993; Brauer *et al.* 1999; Merkt & Müller 1999; Theuerkauf 2003; Baldini *et al.* 2018), volcanologists (e.g. van den Bogaard & Schmincke 1985; Schmincke *et al.* 1999) and archaeologists (Riede 2014). Baldini *et al.* (2018) even discuss the LSE as a possible trigger for the onset of the Younger Dryas (YD).

The LSE is dated to 12 880±40 varve years BP based on the tephra deposition in Lake Meerfelder Maar (Brauer *et al.* 1999; Lane *et al.* 2013; Wulf *et al.* 2013; Bronk Ramsey *et al.* 2015). This is consistent with radiocarbon ages of 12 934±165 cal. a BP (Baales *et al.* 2002) or $^{40}Ar/^{39}Ar$ dates of 12 900±500 years BP (van den Bogaard 1995). The eruption was one of the largest during the late Quaternary in central Europe (e.g. van den Bogaard & Schmincke 1985; Baales *et al.* 2002) and is considered to have been particularly rich in sulphur (Harms & Schmincke 2000).

Several consequences have been considered for the impact of the LSE on contemporary regional environments and people, including ash deposition (Baales *et al.* 2002), acid rain (De Klerk *et al.* 2008), wildfires (De Klerk *et al.* 2008; Engels *et al.* 2015, 2016), increased precipitation (Schmincke *et al.* 1999; De Klerk *et al.* 2008), and cooling (Merkt & Müller 1999; Rach *et al.* 2014; Baldini *et al.* 2018).

A variety of partly contradicting palaeoenvironmental scenarios have been reconstructed regarding the impact of the LSE on central European landscapes. At some sites, the occurrence of severe storms and heavy precipitation events immediately after the LSE was deduced from the sediment records (Merkt & Müller 1999; Schmincke *et al.* 1999). A serious impact of acid aerosols on large parts of central European landscapes has been considered as well (Schmincke *et al.* 1999; De Klerk 2008). Cooling due to the LSE was assumed by Merkt & Müller (1999) and has also been reconstructed based on biomarker analysis (Rach *et al.* 2014). In contrast, De Klerk (2008) found palynological indications of a warming after the end of the Gerzensee oscillation, considered to have occurred simultaneously with the LSE. At a number of sites, a water level increase was reconstructed after the LSE (Theuerkauf 2003). A strong change in the north-Atlantic wind system has been reconstructed to have followed the LSE (Brauer *et al.* 2008). The LSE has recently been considered as the trigger of this changing wind system and consequently

DOI 10.1111/bor.12468

Table 1. Overview of radiocarbon dates and additional age estimates for the Nahe palaeolake sequence. * = the original age estimates given by Litt *et al.* (2007) have been corrected by 110 years to the older considering a hiatus according to Brauer *et al.* (2001); ** = age estimates used in present age-depth modelling.

Radiocarbon dates Lab. no.	Material dated	^{14}C age (a BP) ± 1σ	Master scale (cm)	δ^{13}C (‰ PDB)	Treated as outlier
GrM-17885	Leaf (Poaceae)	15 230±60	1538.95	−17.71±0.2	x
KIA-53569	Branch (undiff.)	11 520±45	1475.7	−29.10±0.2	x
GrM-17289	Branch (undiff.)	10 640±40	1438.8	27.77±0.15	
KIA-53568	Branch (undiff.)	10 445±45	1427.8	−26.60±0.4	
GrM-17841	Branch (undiff.)	10 450±55	1425.3	−27.05±0.2	
KIA-53567	Leaf (*Salix*)	10 450±65	1424.8	−29.70±0.3	
GrM-17288	Fibrillose stem	11 055±40	1424.3	−20.20±0.15	x
GrM-17423	Wood (*Populus*)	11 635±45	1422.3	−27.82±0.15	x
KIA-53566	Wood (*Populus*)	11 650±45	True replicate	−26.40±0.2	x
KIA-53570	Periderm (Pinus)	9650±40	1380.8	−26.00±0.2	
GrM-17242	Root bark	9220±35	1332.8	−24.78±0.15	x
KIA-53565	Root bark	9235±35	True replicate	−24.00±0.2	x
Tephra layers					
Tephra layer	Master scale (cm)	Age estimate (μ + σ cal. a BP)	Reference		
Laacher See Tephra	1465.0	12 937±23	(Bronk Ramsey *et al.* 2015)		
Vedde Ash	1425.0	12 040±35	(Bronk Ramsey *et al.* 2015)		
Saksunarvatn Ash	342.5	10 264±47	(Zanon *et al.* 2019)		
Chronostratigraphical events					
Boundary	Master scale (cm)	Age estimate	Reference		
Pleniglacial/ Meiendorf	1552.0	4560 varve years BP	Corr. after Litt *et al.* (2007)		
Meiendorf/Dryas 1	1524.0	13 910 varve years BP	Corr. after Litt *et al.* (2007)		
Dryas 1/Allerød	1518.0	13 780 varve years BP	Corr. after Litt *et al.* (2007)		
Allerød/Dryas 3	1437.0	12 680 varve years BP	(Litt *et al.* 2007)		
Dryas 3/Preboreal	414.0	1560 varve years BP	(Merkt & Müller 1999)		

has even been assumed as a possible trigger of the onset of the YD cold period (Baldini *et al.* 2018).

An environmental impact is obvious in the areas of the previously known ash fall-out close to the eruptive centre. The Nahe palaeolake, as a very distal site (485 km north of Laacher See), sets a new point on the distribution map of the LSE envelope (Krüger & van den Bogaard 2020). This raises the question whether there is evidence for short-term and direct, i.e. by atmospheric eruptive material, and/or long-term and indirect, i.e. by larger scale climatic responses, impacts on the local environment of distal sites. The presence of the LSE cryptotephra layer within an annually laminated lake sediment sequence at Nahe palaeolake hereby offers the possibility to answer this question with high temporal confidence.

Material and methods

Site

The Nahe palaeolake is located in Schleswig-Holstein (northern Germany) about 30 km north of Hamburg. The former lake basin was part of a larger glacial lake system and is separated from further elongated incision lakes by two narrow sand ridges to the northwest and southeast (Wild 2017). To the southeast, Lake Itzstedt is the water-bearing remnant of the lake system. The geology of the catchment area is composed of glacial deposits (tills, fluvial sands and lacustrine deposits) of the Weichselian glaciation, mainly composed of sediments rich in quartz, with accessory feldspars, mica and clay minerals.

The palaeolake's surface was about 16 ha in size during the Lateglacial. Today, the river Rönne flows in the centre of the still existing depression and thereby follows the course of the former lake towards the northwest and then turning southwards and draining off into the river Alster (Fig. 1). Nowadays, the area is used as pasture and partly forested by alder, birch and willow. The coring location is situated in the formerly deepest part of the lake incision (latitude 53°49′N, longitude 10°08′E). From test corings conducted by Hartmut Usinger in 2003/04 it was clear that the depositional environment of this palaeolake met numerous conditions that are unique in Schleswig-Holstein to date. This includes the facts that (i) the sediments were deposited undisturbed during the entire Lateglacial and Early Holocene, (ii) that they contain an annually laminated section, and (iii) that a Lateglacial cryptotephra was geochemically identified in the sequence Fig. 1 (Krüger & van den Bogaard 2020; Krüger *et al.* 2020).

Fieldwork and sediment sequence

A coring campaign in the centre of the Nahe palaeolake (latitude 53°49′N, longitude 10°08′E) was carried out in

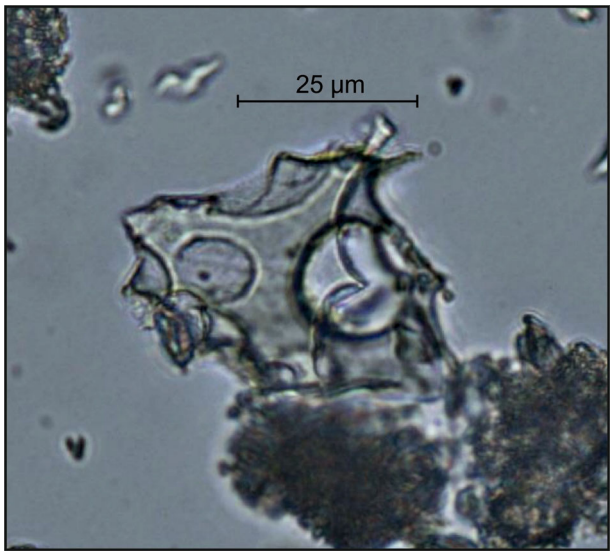

Fig. 1. Microphotograph of the Laacher See cryptotephra detected in the sequences at a depth of 1465.0 cm.

October 2017. A modified Livingston piston-corer (Mingram *et al.* 2007) – the so-called Usinger-corer – was used to extract sequences of 1-m-long sediment cores. Two overlapping sediment sequences with a diameter of 80 mm and a total length of 16 m were recovered. Each 1-m-segment was cut longitudinally and stored in PVC-liners. In order to connect the core sequences, a series of distinct layers and stratigraphical marker horizons were defined in the parallel cores. This way, a composite master sediment record was constructed, representing a continuous sequence avoiding gaps between the individual core segments. As a next step, a subsampling grid of 5-mm step size was created spanning the lower 5 m of the total sequence.

Dating and age-depth modelling

The master sediment record was intensively searched for datable organic material during the subsampling process for pollen and geochemical analysis. A total of 12 botanical macrofossils for AMS ^{14}C dating (including two true replicates) were sent to laboratories in Groningen (GrM) and Kiel (KIA). Additionally, the identification of three cryptotephra layers (Laacher See, Vedde and Saksunarvatn eruptions) in the sediment sequence of Nahe (Fig. 2; Krüger & van den Bogaard 2020) provides three age estimates based on published ages for these chronological event horizons (Bronk Ramsey *et al.* 2015; Zanon *et al.* 2019). Further age estimates are based on the identification of chronostratigraphical palynological events regarded to relate to distinct rapid climatic fluctuations during the Lateglacial period in northern Germany (Table 1).

For the section between 14.93 and 14.45 m, annual laminations allowed the establishment of a floating varve chronology. Varve counting was carried out on thin sections during the microfacies analyses (see below).

An overview of the age information used for the construction of the age-depth model is presented in Table 2. Age-depth modelling was carried out using OxCal v4.3 (Bronk Ramsey 2009) and the IntCal13 calibration curve (Reimer *et al.* 2013). P-sequences (cf. Bronk Ramsey 2008) were used for the unlaminated sections between 1566.5 and 1493.0 cm (lower part) and 1440.0 to 1274.5 cm (upper part), respectively. For the varved section between 1493.0 and 1444.9 cm, a V-sequence was used to anchor the floating varve chronology in terms of the absolute time scale. In order to include information on short-term changes of the sedimentation rate based on the varve chronology in the OxCal model, the Date() function was used to define a date at least every 25 varve years with an associated uncertainty in the gaps of 1. For the additional age estimates based on chronostratigraphical pollen features uncertainties of $\pm$100 years were assigned. Additionally, boundaries were defined in the OxCal model for points at which the sediment composition changes abruptly to allow for associated abrupt changes in the modelled sedimentation rate.

Varve counting and microfacies analyses

Overlapping series of large-scale petrographic thin-sections were prepared for the varved section according to Merkt (1971). Microfacies analysis was carried out using a LEITZ Aristoplan polarization microscope at 25× to 800× magnification under various light and optical conditions. The varves were counted, their thicknesses measured, and the structure of the sub-annual layers (spring, summer–autumn, winter) recorded in accordance with previous microfacies studies on annually laminated lake sediments (e.g. Baier *et al.* 2004; Brauer 2004; Zahrer *et al.* 2013). For the interval *c*. 12 960 to 12 707 cal. a BP, additional sediment components were recorded in detail. The concentration of calcareous shells of *Phacotus lenticularis* (Ehrenberg, Diesing 1866), a species regarded to be sensitive to summer wind conditions, was estimated in semi-quantitative concentration classes ranging from 0 (absent) to 0.75 (blooms, 10% by volume of the sediment) and related to the thickness of the respective layer for the sake of comparability between varves of different thicknesses. The abundance of the green algae *Phacotus lenticularis* is related to water conditions with $CaCO_3$ super saturation and pH > 8.1 (Schlegel *et al.* 1998, 2000; Gruenert & Raeder 2014). Such conditions are common in the littoral zones of temperate hardwater lakes during intensive vegetation growth phases. Planktonic blooms of *Phacotus lenticularis* are restricted to the summer months in field observations in northern Germany (Schlegel *et al.*

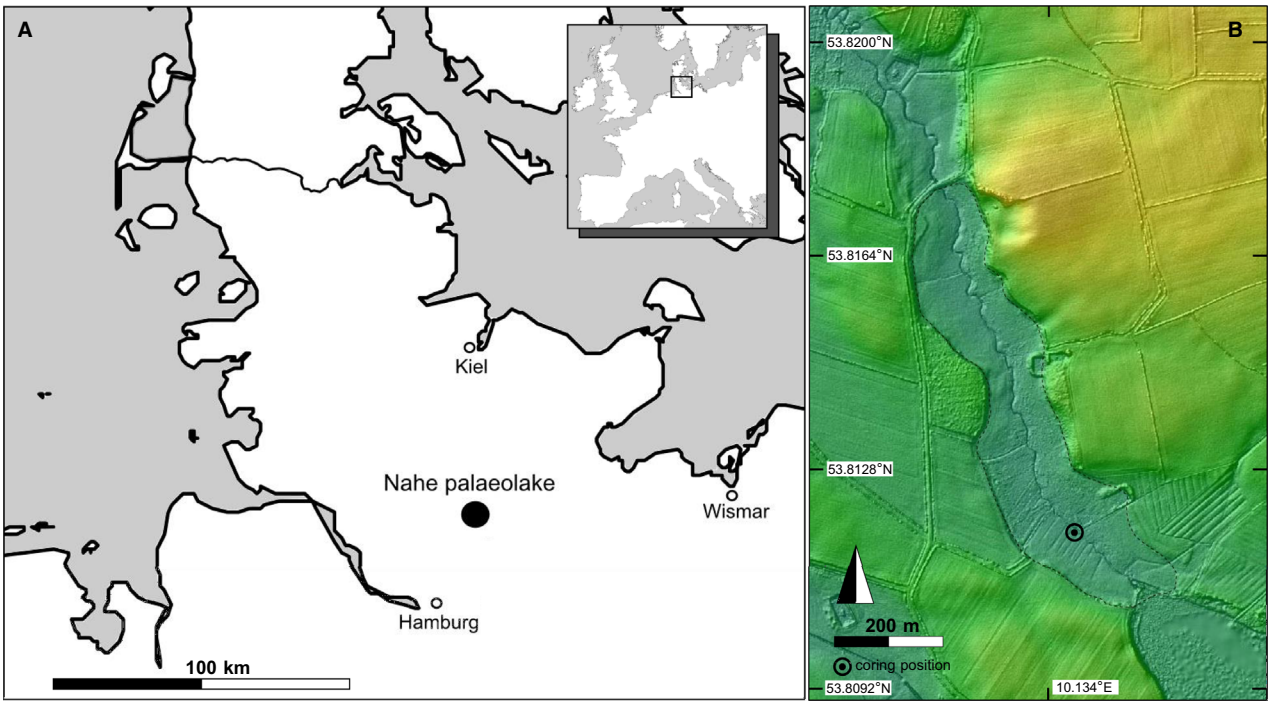

Fig. 2. Geographical location of the Nahe palaeolake in northwest Germany (A) and in Europe (inset) and topographical map (B).

2000). Additionally, the occurrence of hypidiomorphic calcite precipitation layers (spring, summer) was documented.

Varve preservation was recorded using an index ranging from 1 (excellently preserved varve, seasonal sedimentation processes precisely to reconstruct) to 5 (not well-preserved varve, not well developed or disturbed). Statistical analyses (e.g. REDFIT time series analysis) on varve thickness data were carried out using PAST software (version 2.06, Hammer *et al.* 2001).

Water content, bulk density, total elemental contents

Water content (WC) and dry density (DD) of the sediment deposited during the Allerød and YD were determined gravimetrically after drying volumetrically continuous 0.5-cm increment samples in a vacuum dryer. Following homogenization, the total and minor elemental contents were determined using a p-ed-XRF device (Niton XL3t900). The measurements were carried out with He-flotation in the measurement chamber of this device using the 'mining, Cu/Zn' settings for 300 s. All elements measured with an error of >10% according to the device were discarded from further analysis. Correction factors published in Dreibrodt *et al.* (2017) were used to convert the semi-quantitative % values as displayed by the device into % by weight values.

Total carbon (TC), total nitrogen (TN) and total inorganic carbon contents (TIC) were measured for the varved sediment section following the LSE on a Euro EA-CHNSO Element Analyzer. Total organic carbon (TOC) contents were calculated by subtracting TIC from TC.

Based on the chronology and dry density of the sediments, the sediment accumulation rate (SAR) was calculated (g cm^{-2} a^{-1}). Elemental contents were converted into fluxes according to that SAR.

Pollen analysis

Pollen sampling, preparation and counting techniques follow standard protocols (Erdtman 1960; Fægri & Iversen 1989; Beug 2004) and are described in detail in Krüger *et al.* (2020). Reported influx values (pollen accumulation rates) were calculated based on the sedimentation rate (cm a^{-1}) as derived from varve counting.

Results and interpretation

Chronology

The results of the age-depth modelling are presented in Fig. 2. Seven of the available 12 radiocarbon dates revealed too old ages in the context of other available age estimates, i.e. anticipated ages for the known volcanic eruptions and 'pollen-stratigraphical' features. Accordingly, these radiocarbon dates were interpreted as outliers, probably relating to reworked secondary material. The dating of the lower non-laminated part (NAH P_Sequence lower part in Fig. 2) therefore relies only on

Table 2. Comparison and definition of chronostratigraphical palynological features of the Nahe palaeolake sequence with biochronological events for northern Germany.

Terminology NAH	Terminology MFM (Litt *et al.* 2007)	Age estimate	Features of NAH PAZ boundaries
Preboreal	Preboreal		*Betula pub.*-type ↑, *Filipendula*, *Typha lat.*-type ↗, Poaceae, *Artemisia*, *Empetrum*, other NAP-types↘
		(11 560 varve a BP)**	
Dryas 3	Younger Dryas	(Merkt & Müller 1999)	*Betula pub.*-type ↘, *B. nana*-type, Poaceae, *Artemisia*, other NAP-types ↗
		(12 680 varve a BP)**	
Allerød 3	Allerød/	(Litt *et al.* 2007)	*Betula pub.*-type ↗, *Juniperus*, Poaceae, other NAP types ↘
		(13 350 varve a BP)	
Allerød 2/ Dryas 2	Older Dryas	(Litt *et al.* 2007)	*Betula pub.*-type ↘, *Juniperus*, Poaceae ↗
		(13 650 varve a BP)	
Allerød 1	Bølling	(Litt *et al.* 2007*)	*Betula pub.*-type ↑, *Hippophaë* ↗ Poaceae, *Helianthemum* ↘
		(13 780 varve a BP)**	
Dryas 1	Oldest Dryas	(Litt *et al.* 2007*)	*Hippophaë*, AP ↘, Poaceae, *Helianthemum*, *Rumex acet.*-type ↗
		(13 910 varve a BP)**	
Meiendorf	Meiendorf	(Litt *et al.* 2007*)	*Pinus* ↘, *Betula pub.*-type, *B. nana*-type, *Artemisia*, *Hippophaë* ↗
		(14 560 varve a BP)**	
Pleniglacial	Pleniglacial	(Litt *et al.* 2007*)	

'pollen-stratigraphical' synchronization. The upper non-laminated part (NAH P_Sequence upper part), however, is constrained by four radiocarbon dates, the dating of the Saksunarvatn tephra event as dated by Zanon *et al.* (2019) and two 'pollen-stratigraphical' features representing the end of the Allerød and the Younger Dryas periods, respectively. The chronology of the varved section (NAH V_Sequence) mainly relies on the floating varve chronology fixed by the dating of the Laacher See eruption according to Bronk Ramsey *et al.* (2015). According to the model the varved sequence spans the younger part of the Allerød period starting at 13 421 cal. a BP (2 sigma range 13 464–13 378±43 cal. a BP) and ending at 12 708 cal. a BP (2 sigma range 12 751–12 665±43 cal. a BP). In the following, all ages relating to the Nahe sediment sequence refer to the modelled median ages of the presented age-depth model.

Geophysical and geochemical sediment analyses

Water content (WC) and dry density (DD) curves are given in Fig. 3. The diagrams span the interval from the Dryas 1 period to the Preboreal period. In general, the cool climatic periods are characterized by lower WC and higher DD values. The Allerød section contains a generally higher water content and a lower dry density compared to the remaining sediment sequence. This reflects changes of the sediment composition between warmer and cooler climatic periods. In both curves, there is a trend towards maximum values of WC and minimum values of DD between 13 200 and 12 900 cal. a BP. Following the LSE, a trend towards lower WC and higher DD values is visible. A pronounced step with lower WC and higher DD values characterizes the transition to the YD.

Sediment accumulation rates (SARs) were calculated for the varved part of the sediment sequence (Fig. 3). A general trend of increasing values is visible throughout the Allerød period. Between 13 180 and 13 090 cal. a BP a secondary maximum of SAR is visible.

Varve analyses

Varve preservation. – The preservation of varves is displayed in Figs 5 and 9. The varve preservation throughout the Allerød is varying. Most varves are preserved in a moderate condition. The variability of the varve preservation is different in the pre- and post-LSE sections of the Allerød period.

Varves of the pre-LSE section are generally preserved in a moderate condition (varve preservation index generally between 3–4) except between *c.* 13 160–13 120 cal. a BP and after *c.* 13 040 cal. a BP, where there is generally better preservation (varve preservation index generally between 2–3). After the LSE, between *c.* 12 930 and 12 840 cal. a BP a high variability and generally lower level of varve preservation prevail including three small non-varved sections. Microscopical inspection gave no indications of an extraordinary input event or lake internal slump of sediments. Instead, a faint layering of the main components (carbonates, organic detritus) is present.

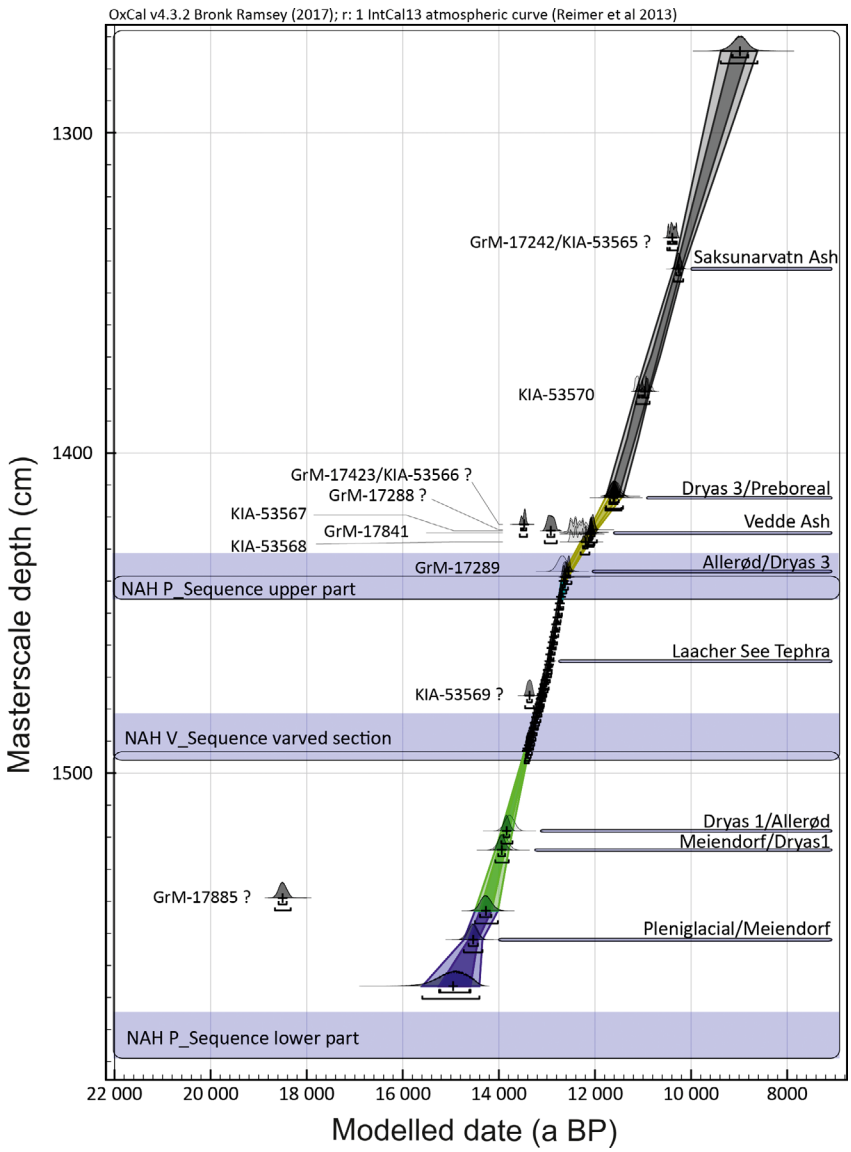

Fig. 3. Age-depth model of the Nahe palaeolake sediment sequence. Labels of radiocarbon dates are given to the left of the age-depth curve. Dates treated as outliers are marked with question marks. Level and names of additionally used age estimates, i.e. volcanic eruptions and 'pollen-stratigraphical' events, are indicated on the right side of the age-depth curve. Different coloured sections represent differentiated stratigraphical units separated by the Boundary () function in the OxCal model (Bronk Ramsey 2009).

Therefore, the mean thicknesses of the foregoing and following five varves were used to interpolate the sedimentation of the non-varved sections. The remaining varved section (*c.* 12 840–12 707 cal. a BP) shows medium to good varve preservation that ends abruptly towards the YD transition.

Varve counting. – Varve counting of the 205-cm-thick laminated interval yielded a duration of 716 years, including three short sections without varve preservation. These non-varved sections date to the late Allerød period after the LSE and have thicknesses of ~6, 9 and 2 mm. The microscopical analysis revealed no indication of strong disturbance (slump), but instead a faint layering. Thus, the sedimentation rates were extrapolated based on the average of the five foregoing and following varves to reflect deposition periods of 7, 12 and 4 years respectively. These interpolated 23 years make up less than 4% of the total varve number and thickness of the sequence and are thus not considered to change the chronology significantly.

Varve thickness. – Varve thickness is displayed in Fig. 3. The average and median varve thicknesses measure 0.64 and 0.57 mm, respectively, with a minimum of 0.20 mm and a maximum of 4.35 mm. While showing some variability there is a long-term trend of growing varve thicknesses throughout the Allerød (Fig. 3).

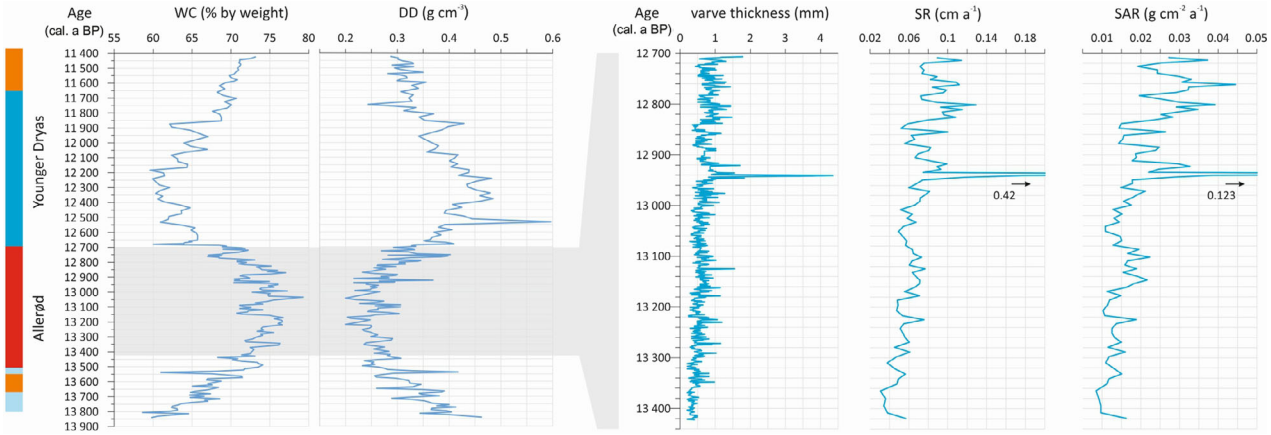

Fig. 4. Allerød and Younger Dryas section of the Nahe palaeolake sediment sequence. Left: water content (WC) and dry density (DD); right: varve thickness, sedimentation rate (SR) and sediment accumulation rate (SAR).

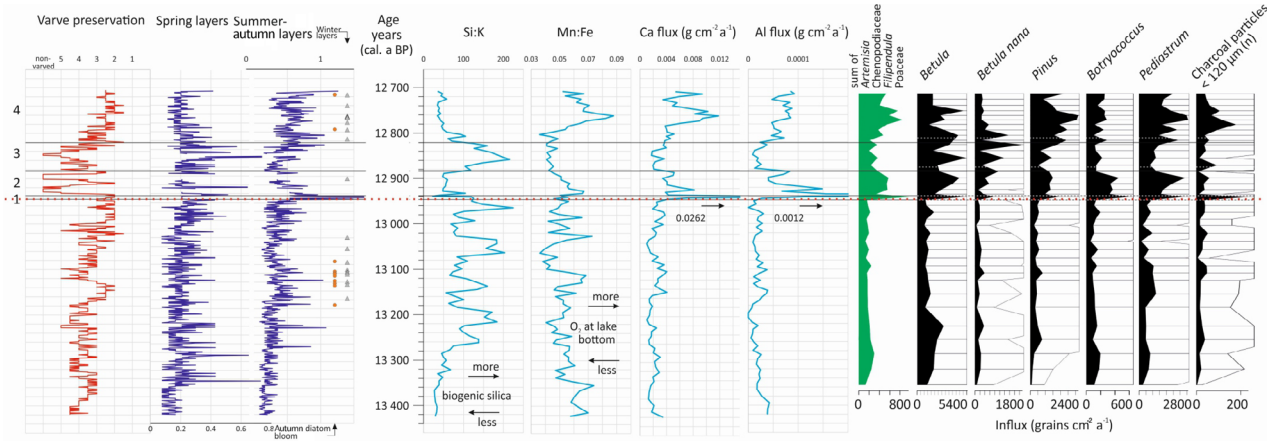

Fig. 5. Selected results of microfacies analysis, geochemical measurements and influx rates of pollen and spores from the annually laminated Allerød sequence of the Nahe palaeolake sediment sequence: varve preservation from 1 (excellent) to 5 (non-varved), varve thickness in mm of spring and summer–autumn layers in mm, Si:K ratio, Mn:Fe ratio, Ca- and Al-flux (g cm^{-2} a^{-1}); influx rates of selected pollen and algal types, number of micro-charcoal particles per sample (<120 µm).

Within the subsampling range of the identified Laacher See cryptotephra (1463.5–1465.5 m) a series of extraordinarily thick varves were recorded (1465.0–1462.9 m, mean 1.8 mm, median 1.3 mm). Particularly the lowermost varves exhibit thicknesses considerably greater than usual (1.67, 3.46, 4.31 and 2.52 mm). According to the age-depth model, they date to the years 12 943–12 940 cal. a BP and are therefore interpreted to reflect the years directly after the LSE. A pronounced minimum of varve thickness is present between 12 854 and 12 839 cal. a BP. Subsequently varve thickness shows generally higher values (mean 0.86 mm) compared to the mean Allerød values.

A REDFIT time series analysis was applied to the varve thickness data (Schulz & Mudelsee 2002). Because of the presence of poor and non-varved parts after LSE, the analysis was restricted to the pre-LSE part of the Allerød sequence (from 13 371 to 12 894 cal. a BP). Figure S1 displays short cycles (2–3, 8 and 62 years), which could reflect a response of the lake system to the North Atlantic climate variability (NAO and AMO). Longer cycles (93.2 and 99.2 years) could reflect the impact of solar activity on the lake system (Gleissberg cycle, e.g. Peristykh & Damon 2003). The identification of cycles reflecting known climatic variability supports the quality of the established chronology and the sensitivity of the sequence to external triggers.

Varve composition. – The varves show a general structure similar to Holocene calcareous biogeochemical varves of hardwater lakes (e.g. Zahrer *et al.* 2013). These consist of a spring biogenic silica layer followed by a carbonate layer assumedly reflecting summer to early autumn epilimnic carbonate precipitation. This merges with the autumn deposition containing resuspended littoral material and organic matter (cf. Fig. 6). In some

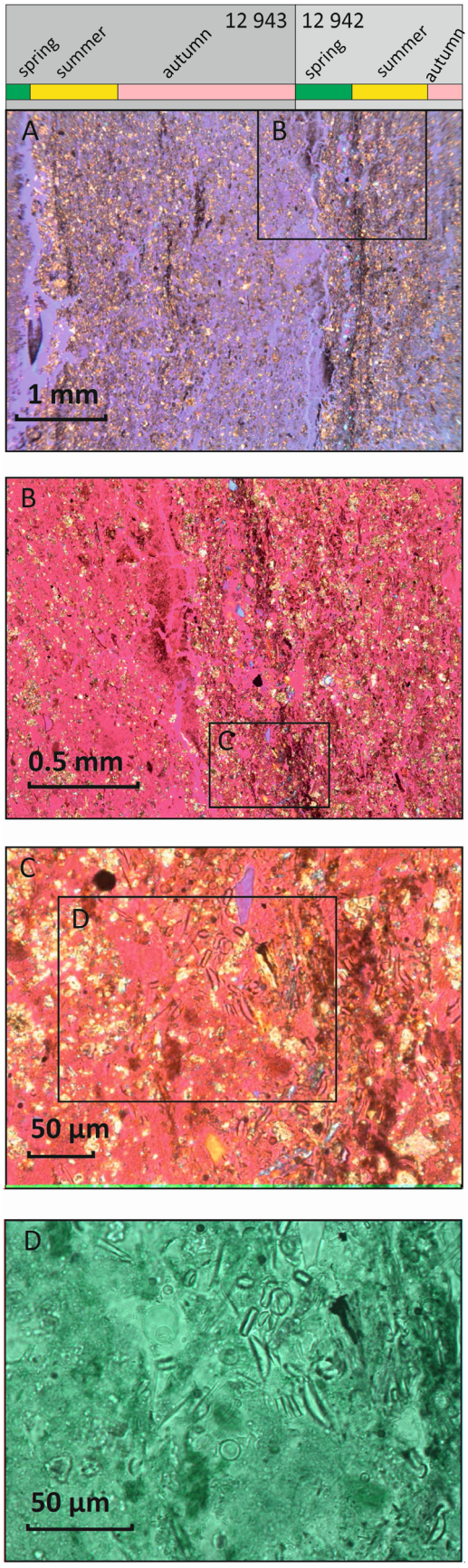

Fig. 6. Microphotographs of the varves dating to 12 943 and 12 942 cal. a BP. A–C. Crossed Nichols, lambda red filter; D. Non-polarized light. A. Overview showing the annual sequence of year 12 943 on the left: spring (clear blue, one large littoral bio-remain), summer (rich in calcite), autumn (resuspended mixture including organic remains) followed by spring, summer, and the initial part of the autumn layer of year 12 943. B. The autumn of year 12 943, spring, summer and initial part of autumn of year 12 942; note the layer of detrital input (quartz grains) in the late spring layer. C. Spring of the year 12 942; note calcite precipitation, detrital grains (quartz) and diatoms, followed by organic detritus and carbonate minerals of the summer layer. D. Diatom frustules preserved in the spring layer of year 12942 (*Stephanodiscus* spec., *Cymbella* spec., *Fragilaria* spec.).

varves, autumn diatom blooms have resulted in the deposition of a biogenic silica layer. Very rarely, thin fine detritus-rich layers reflect the preservation of winter layers. The varve sub-annual composition is given in Figs 5 and 9. The spring layer thickness exhibits considerable variability. From *c.* 13 340 to 12 780 cal. a BP, the spring layers are thicker in general. Maxima of phases coincide with high Si:K ratios of the sediment. The most pronounced variability in spring layer thickness occurs after the LSE. The variability in summer–autumn layer thickness is most pronounced after the LSE. Despite this long-term trend, a phase of increased summer–autumn layer thickness is recorded between *c.* 13 160 and 13 080 cal. a BP. After the LSE, the most pronounced variability in summer–autumn layer thickness is visible. Occurrences of autumn diatom blooms are limited to the intervals between 13 185–13 080 cal. a BP and after the LSE (orange circles in Figs 5 and 9). Winter layers are preserved between *c.* 13 180–13 040 cal. a BP and after the LSE (grey triangles in Figs 5 and 9).

Except for a very few years, no intact diatom frustules are preserved in the varves. Instead, a layer of silica gel is preserved, similar to that described by Merkt & Müller (1999). Poor diatom preservation is a well-known feature of Lateglacial to Early Holocene sediments (e.g. Smol & Boucherle 1985; Newberry & Schelske 1986). It is considered to reflect diatom frustule dissolution in higher lake-water pH at the time of carbonate deposition. The presence of the silica gel layer in the micro-stratigraphical position below the carbonate rich layers throughout the sequence indicates that diatom frustule dissolution was a seasonal phenomenon followed by re-precipitation of the opal at the lake bottom. The stratigraphical position of the silica gel layer further indicates a regular deposition following the spring planktonic diatom blooms during the early part of the summer stratification. The development of anoxic conditions at the beginning of summer stratification probably resulted in the annual re-precipitation of the silica gel at the lake bottom by promoting lower pH conditions.

In the four extraordinarily thick varves deposited immediately after the LSE, however, diatom valves are preserved (Fig. 6). The valves are embedded in a matrix rich in silicate minerals that originated from allochtho-

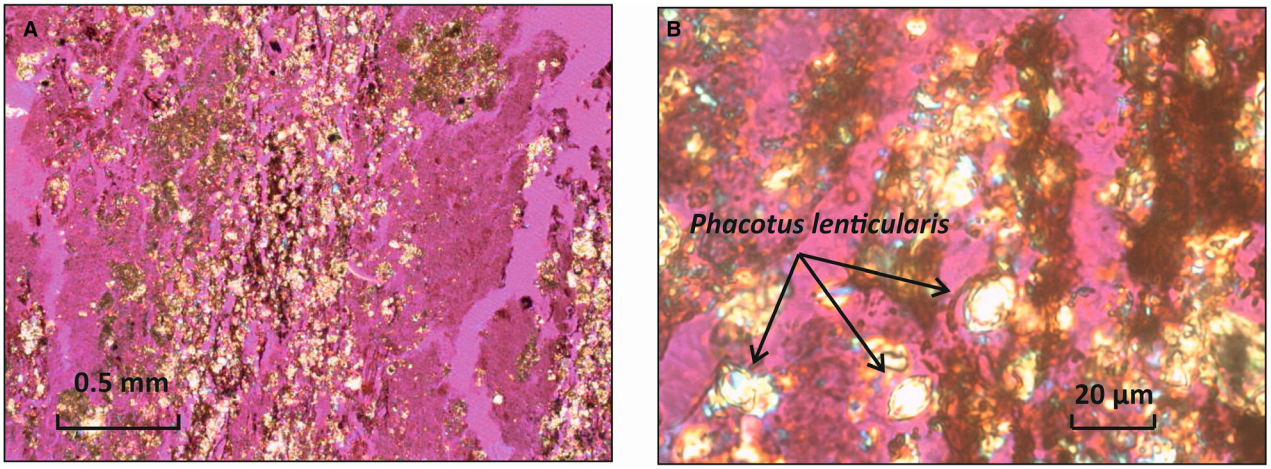

Fig. 7. Calcareous shells of the green algae *Phacotus lenticularis* in varve year 12 911 cal. a BP; crossed Nichols, lambda red filter. A. Overview of year 12 911, spring layer (amorphous silica gel), summer layer (carbonate precipitation, micritic/detrital mixture), late summer/early autumn layer (organic detritus/carbonate mixture), autumn layer (resuspended mixture, including some striatal grains), followed by the spring layer (amorphous silica gel) of year 12 912. B. Shells of *Phacotus lenticularis* embedded in the mixture of organic detritus and carbonates of the late summer/early spring layer.

nous input into the lake. A higher amount of allochthonous detrital minerogenic input is visible in the autumn layers as also described by Merkt & Müller (1999). Therefore, the preservation of frustules in the four varves after the LSE was probably favoured by a higher amount of silica solute in the lake's water body. In the second varve year after the LSE an increased input of quartz grains is visible in the spring season, perhaps reflecting soil erosion due to a high-energy rainfall event in the catchment area. The preserved diatom assemblage deposited on top of this allochthonous input layer contains a large amount of planktic diatoms, thus reflecting remains of a spring plankton bloom.

The abundance of the green algae *Phacotus lenticularis* (Fig. 7) is related to water conditions with $CaCO_3$ super saturation and pH > 8.1 (Schlegel *et al.* 1998, 2000; Gruenert & Raeder 2014). Such conditions are common in the littoral zones of temperate hardwater lakes during intensive vegetation growth phases. Since planktonic blooms of *Phacotus lenticularis* are restricted to the summer months in field observations (Schlegel *et al.* 2000) and their shells are made up of calcite, blooms are probably also related to wind conditions during the summer time. Windier summer seasons with higher turbidity should allow the relatively heavy shells to stay longer in the epilimnion than less windy summer seasons.

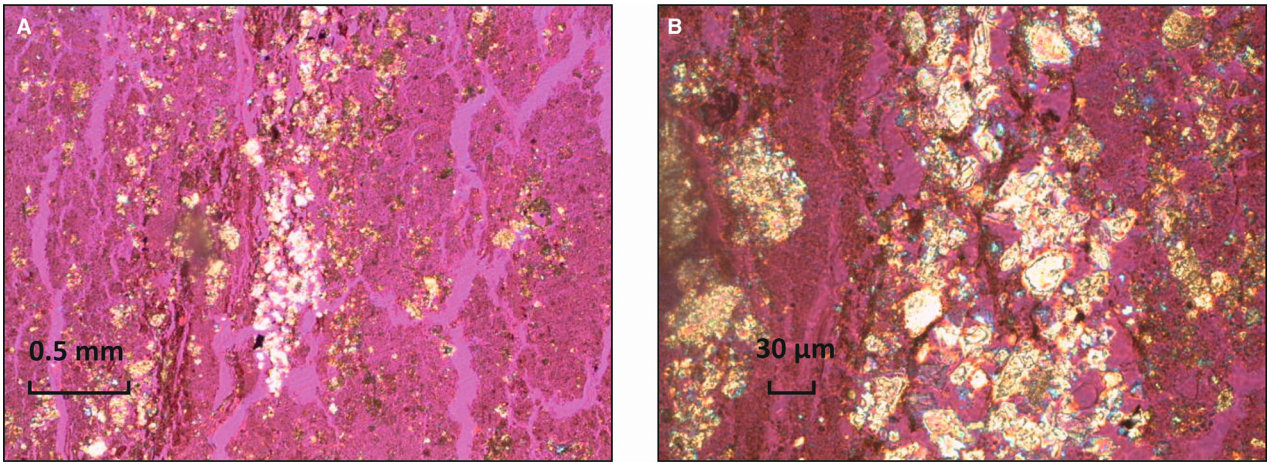

Fig. 8. Hypidiomorphic spring calcite crystals of varve year 12 854 cal. a BP; crossed Nichols, lambda red filter. A. Overview of year 12 953, autumn layer (mixture of calcite, detritic organic matter), and 12 954 spring layer 1 (amorphous silica gel), spring 2/early summer layer (hypidiomorphic carbonate precipitation), late summer/early autumn layer (micritic carbonate/detrital mixture), autumn layer (organic detritus/carbonate mixture). B. Hypidiomorphic calcite crystals of a diameter between <10 and 30 µm in the late spring/early summer layer.

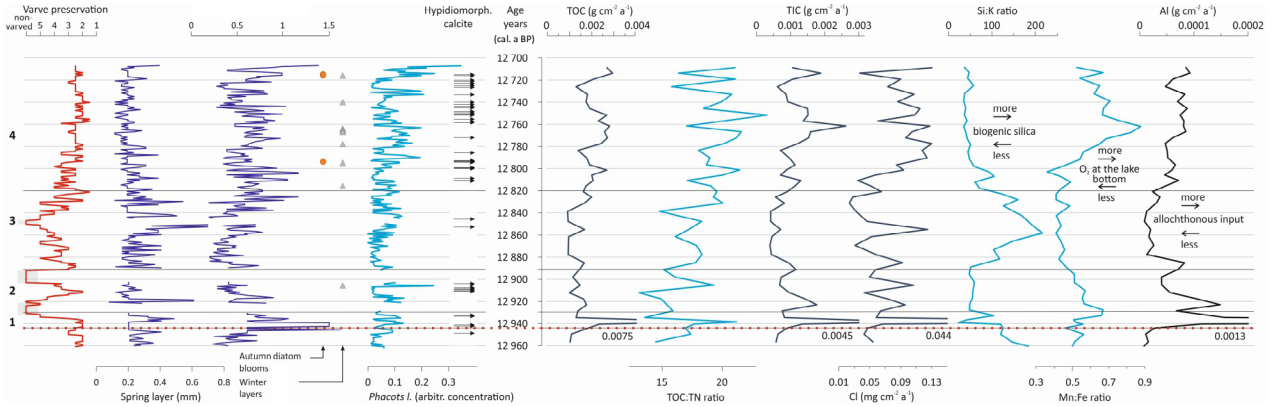

Fig. 9. Selected results of microfacies analysis and geochemical measurements from the annually laminated sediments deposited after the LSE. Varve preservation from 1 (excellent) to 5 (non-varved), concentration of shells of *Phacotus lenticularis* (arbitrary concentration units related to layer thickness), occurrence of hypidiomorphic calcite crystals in the spring/early summer layers; accumulation rates of TOC, TIC, Cl and Al, ratios of TOC:TN (allochthonous vs. autochthonous organic matter), Si:K (biogenic silica) and Mn:Fe (aeration of the lake bottom).

The concentration of shells of *Phacotus lenticularis* shows an increasing trend in the post-LSE period although with considerable variability (Fig. 9). Increased concentrations hereby coincide with higher TIC, Cl, and the occurrence of larger hypidiomorphic calcite precipitation in the sediment.

The occurrence of coarse-grained hypidiomorphic calcite crystals (Fig. 8 and indicated by lateral arrows in Fig. 9) precipitated in the epilimnion is considered to reflect enduring turbulent water conditions during crystal growth (e.g. Kelts & Hsü 1978; Prasad *et al.* 2007; Czymzik *et al.* 2016). Large hypidiomorphic calcite crystals occur immediately after the LSE and in the following interval more regularly from 12 812 varve years BP to the end of the preserved varved sequence. The hypidiomorphic crystals co-occur with higher fluxes of Cl, Al and *Phacotus lenticularis* into the sediment as well as a higher Mn:Fe ratio.

Geochemical sediment analyses

The total elemental contents of the Allerød sediment sequence are given in Table S1. A correlation matrix is given in Table S2. The strongest positive correlation exists between Ca and Sr underlining their co-occurrence in carbonates in lake sediments. The strongest negative correlations are observed between Fe and Ca and Fe and Sr, respectively. This might indicate a relationship between bioproductivity and precipitation of carbonates in the lake system. Hereby, a high level of bioproductivity could have induced oxygen consumption at the lake bottom during the decomposition process of organic matter, in turn causing more reducing conditions at the lake bottom unfavourable for Fe immobilization. The correlations of Si with Al, K and Zr are rather weak, indicating that a certain amount of the Si is not bound to allochthonous minerogenic particles but of biogenic origin. The positive correlation of Si with Fe, and the negative correlations between Si and Ca and Sr, indicate that amorphous silica re-precipitation is related to redox and alkalinity conditions at the lake bottom. An overview of indicative elemental ratios and flux rates is shown in Figs 5 and 9. Si content of lowland lake sediments is related to two main sources. These are catchment and shore erosion and biogenic silica (mainly diatoms). Thus, the content of excess Si (biogenic silica) is often evaluated using ratios between Si and other elements abundant in catchment minerals but not in diatom valves, e.g. Si:Ti (e.g. Kylander *et al.* 2011). Since the Ti values are below detection limits in our sequence, we could not use the Si:Ti ratio as a proxy for biogenic silica here. Instead, the Si:K ratio (Figs 5, 9) is considered to reflect the variability of Si unbound in minerals and thus is a proxy for the biogenic silica content of the sediment. K is considered here as a rather conservative element that mainly reached the lake with allochthonous input (muscovite, illite, feldspars). The pattern of the Si:K ratio of the sequence shows high similarity to the Si:Al and Si:Zr ratios (Table S1), which both are also likely to reflect mainly the variability of excess Si (biogenic silica). Whereas the biogenic silica content of the sediment is in general higher during the interval from *c.* 13 000 to 12 800 cal. a BP than before and after, considerable variability is visible in the record. The curve displays a quasi-cyclicity with alternating minima and maxima of biogenic silica deposition with cycle lengths of 50–80 years, typical for the Atlantic Multidecadal Oscillation (AMO, e.g. Kerr 2000). Immediately after the LSE, there is a drop to low Si:K levels. Subsequently, about 60 to 120 years after the LSE, high Si:K values reflect higher amounts of biogenic silica deposition again, before biogenic silica deposition decreases and remains low until the end of varve preservation.

The Mn:Fe ratio (Figs 5, 9) reflects the oxygen conditions at the lake bottom (e.g. Wersin *et al.* 1991; Naeher *et al.* 2013). In general, the Mn:Fe ratio shows lower values during the interval from *c.* 13 000 to

12 800 cal. a BP compared to the previous and subsequent phases. This probably reflects a higher content of organic components in the Allerød sediment sequence. The decomposition of the organic matter would explain more intensive oxygen consumption at the lake bottom. The LSE is followed by a short increase in the Mn:Fe ratio, before a trend to lower values is visible for about *c.* 120 years. This is followed by a steep increase in the Mn:Fe ratio culminating in a maximum at *c.* 12 760 cal. a BP. Towards the end of varve preservation a slight decrease to moderately high values can be observed.

The Ca flux rate (Fig. 5), interpreted to represent the accumulation of $CaCO_3$, shows only little variability during the Allerød period before the LSE. Increased Ca and Al accumulation between *c.* 13 160–13 080 cal. a BP coincides with a maximum in Si:K between 13 140–13 120 cal. a BP followed by a maximum of Mn:Fe ratios as well as with poorer preservation of thinner varves until *c.* 13 100 cal. a BP. This sedimentation pattern could indicate higher wind speed conditions leading to increased carbonate precipitation (e.g. Czymzik *et al.* 2016). Statistical analysis of weather and surface wave data from Lake Woserin, northern Germany, spanning the past 70 years indicates this effect was probably related to higher numbers of seed crystals and a longer growth time of calcite particles in more turbulent surface water, additionally to increased in-wash of Ca. The time after the LSE is characterized by distinctly increased variability of the Ca flux rate reflecting rapidly changing sedimentation dynamics. A pronounced maximum of Ca accumulation is reached immediately after the LSE, followed by a stepwise decrease. A distinct minimum is observed between 12 880 and 12 840 cal. a BP. Afterwards moderate Ca accumulation rates (12 840–12 780 cal. a BP) are visible, followed by a steep increase to a secondary maximum of Ca accumulation between 12 780 and 12 740 cal. a BP.

Similarly to the Ca flux rate, the Al flux rate (Figs 5, 9), interpreted to reflect allochthonous minerogenic input, shows rather little variability over large parts of the Allerød before the LSE. Although there is some increase of Al accumulation between *c.* 13 160 and 13 080 cal. a BP, this is clearly exceeded by maximum values that occurred after the LSE.

The Cl flux curve (Fig. 9) may reflect the deposition of chlorine from different sources. They might be of marine (aerosols) or geological origin. Whereas salt diapirs (Zechstein) are known to exist as extended subsurface geological structures in northern Germany, in very few cases the Zechstein rocks reach the surface. One is located close to the city of Elmshorn, 40 km west of the investigated palaeolake (e.g. Schneider & Gebhardt 1995). Thus, the Cl accumulation observed in the NAH sequence is probably associated with the strength of westerly winds, either reflecting the input of aerosols from the Atlantic-maritime air masses or from the small known exposure of Zechstein rocks.

Pollen accumulation rates

The influx curves for selected pollen, algal remains and charcoal particles are given in Fig. 5. A sum curve of selected non-arboreal pollen (NAP) includes pollen types identified as *Artemisia* sp., *Filipendula* sp., Chenopodiaceae and Poaceae. There is some noticeable variability in the influx rates of terrestrial plant pollen and algae in the displayed part of the pre-LSE Allerød. Higher influx values of *Betula* occurred between 13 360 and 13 200 cal. a BP. Afterwards, until the LSE, the influx values of *Betula* are lower. *Pinus* appears with a moderate influx value at *c.* 13 260 cal. a BP and remains at a low level with little variability. The influx of the green algae *Pediastrum* sp. shows higher values between 13 160 and 13 080 cal. a BP, paralleling the trends in Ca and Al accumulation. Some peaks of charcoal input occurred between 13 120 and 13 080 cal. a BP and 13 040 to 13 000 cal. a BP. Compared to this pre-LSE variability, however, an overall significant shift towards higher influx values is apparent immediately after the LSE.

Discussion

Palaeolimnological and -environmental changes before the LSE

Varve microfacies analysis and geochemical data of the Allerød sequence from the Nahe palaeolake imply rather continuous lake sedimentation processes in a dynamic equilibrium with the interstadial conditions prior to the LSE.

The shift in the sediment composition between *c.* 13 160 and 13 080 cal. a BP, increased Ca and Al accumulation (Fig. 5) and lower WC and higher DD (Fig. 3), are regarded to reflect a local response to cooling and increased average wind speed related to the Gerzensee oscillation (e.g. Lowe *et al.* 2008; von Raden *et al.* 2013). The observed increase in carbonate precipitation and input of Al coincides with the occurrences of autumn diatom blooms and winter layers and probably is the result of increased in-wash and/or shore erosion (cf. Czymzik *et al.* 2016). The parallel increase of the *Pediastrum* curve (Fig. 5) therefore most likely indicates enhanced nutrient availability. The observed pattern is in good agreement with the assumption of a phase with cooler than usual winters and windier than usual conditions during the vegetation growth period. The recurrence of prior sedimentation conditions and the persistence of reflected Atlantic patterns within the record (cf. results for biogenic silica in Geochemical sediment analyses section) imply a response of the lake system to climate variability that does not distinctly cross the thresholds of the system's vulnerability.

In comparison, limnological changes after the LSE are much more pronounced. Changes in the sediment record, including short interruptions of varve preservation, imply a serious disturbance of the lake system triggered by the LSE.

Palaeolimnological and -environmental changes after the LSE

As this paper focusses on the local palaeolimnological and -environmental changes after the LSE the developments between 12 944 and 12 707 cal. a BP as recorded in the Nahe record are in the following described and discussed in four phases. These phases have been defined based on coinciding distinct changes in multiple proxies and therefore are regarded to represent phases of different palaeoenvironmental conditions.

Phase 1 (12 944–12 930 cal. a BP). – This phase is characterized by the onset of a series of extraordinarily thick varves (12 943–12 940 cal. a BP), mainly due to increased thickness of the summer–autumn layers (mean 1.60 mm, max. 4.35 mm, min. 0.81 mm). High accumulation values of Al and a discrete layer rich in quartz grains in the second year after the LSE point to a serious storm or erosion event within the catchment area. This might indicate stormy seasons and/or local heavy precipitation events that immediately followed the LSE (e.g. Merkt & Müller 1999; Schmincke *et al.* 1999). The immediate and synchronous rise in PAR and in particular charcoal influx probably reflects changed pollen introduction into the lake and could likewise be explained by extreme weather events that plausibly mobilized material in the shore area and catchment of the lake.

To conclude, the results indicate serious disturbance of the local environment immediately after the LSE.

Phase 2 (12 929–12 893 cal. a BP). – The sediment record of Phase 2 consists of two non-laminated sections between 12 929–12 913 and 12 902–12 893 cal. a BP with a laminated part in between, indicating variable sedimentation conditions. It is characterized by low Si:K and high PAR values. A distinctly increased minerogenic content is furthermore indicated by a lull in the water content (WC) and high dry density (DD) values (Fig. 3). Compared to pre-LSE conditions the Al and Ca accumulation rates remain at an elevated level, although a trend towards lower values is recorded. A similar trend is observed for the Mn:Fe ratio. Indicators of aquatic biogenic productivity such as TOC and the Si:K ratio have low values (Fig. 9), whereas the accumulation rates for green algae (*Botryococcus* sp., *Pediastrum* sp.) are increased, in a context of generally high PAR values (Fig. 5). The TOC:TN ratio of the deposited organic components shows a clear drop with the beginning of Phase 2 and low values prevail until *c.* 12 905 cal. a BP. Afterwards TOC:TN increases sharply. This increase seems to be associated with more undisturbed sedimentation processes in the middle of Phase 2, i.e. represented by the section with preserved varves between 12 922–12 903 cal. a BP. This section is further characterized by local minima of the Al and Ca accumulation rates and regular records of hypidiomorphic carbonate crystals.

The low biogenic silica deposition, as reflected in low Si:K values coinciding with low TOC accumulation and low TOC:TN ratios, could reflect an acidification of the lake water during Phase 2. This seems reasonable because the LSE is known to have been a sulphur rich eruption (Harms & Schmincke 2000) and acidification effects on lakes have been described for other strong volcanic eruptions as well (e.g. Grattan & Charman 1994). The drop in biogenic silica, as expressed in the Si:K ratio, and the thinner varves are interpreted to reflect decreased diatom productivity. Diatoms are pH sensitive and have been intensively used as proxies for lake water acidification (Battarbee *et al.* 1984, 1999). The assumed acidity related drop of diatom productivity could partly explain the occurrence of the two small non-laminated sections, since the biogenic silica layer constitutes a main component of the varves. The low TOC:TN ratio before 12 905 cal. a BP is thus not interpreted to indicate eutrophication (e.g. Meyers 1994; Meyers & Ishiwatari 1995) but might rather reflect that mainly acid tolerant algae groups of phytoplankton contributed to the aquatic bioproductivity. The higher influx values of the green algae *Botryococcus* sp. and *Pediastrum* sp. that parallel the low amount of biogenic silica partly reflect the shift in dominant algal groups following an acidic input (Weckström *et al.* 2010).

The recorded short-term response of the Nahe palaeolake system to the LSE is in accordance with acid rain fall-out and events of intense precipitation reported from other sites in northwestern Europe (Schmincke *et al.* 1999; De Klerk 2008). Since lake acidification changes the aquatic food web to a major extent, including shifts of fish species and their abundances, relevant to early fisherman, might be considered (e.g. Hogsden *et al.* 2009).

The sinking Mn:Fe ratio indicates decreasing oxygen concentration to the lake bottom. Less oxygen at the lake bottom could result from eutrophication, lowering in wind speed, and lake level increases. The former two can be excluded considering the indications of lower aquatic bioproductivity and allochthonous input into the lake. The high pollen influx rates during Phase 2 point towards the same direction. They probably result from increased in-wash or increased sediment focussing in the deeper part of the lake, due to increased redeposition of littoral sediments (Davis 1968, 1973; Davis & Ford 1982). A lake level rise would explain the declining Mn:Fe ratio in the context of increased accumulation rates for Al, palynological microfossils and terrigenic organic matter (TOC:TN) in the deeper part of the lake basin associated with shore erosion and/or redeposition of littoral sediments.

The geomorphic setup of glacial lakes in the northern European plain allows a lake level rise only (i) until a certain threshold is reached (outflow barrier), and (ii) if the lake level was below that threshold before. The chemical composition of Lateglacial sediments, which is often found to be enriched in readily soluble elements (e.g. sulphur) and alkaline minerals (e.g. siderite), points towards the presence of closed lake systems during the Lateglacial period (Smol & Boucherle 1985; Newberry & Schelske 1986; Merkt & Müller 1999). The contents of S and P in the studied sediment sequence (particularly the pre-LSE sediment) are much higher than those observed in sediments of Holocene open lake systems with inflow and outflow (Table S1). Thus, it is very possible that the Nahe palaeolake had no outlet during large parts of the Allerød, and a lake level increase up to the geomorphological barrier of the basin occurred after the LSE. Water level increases are reported from wetland areas in northeastern Germany following the LSE (e.g. Lange *et al.* 1986; Peterss *et al.* 2002; Theuerkauf 2003). Evidence for a decrease in temperature as assumed by Merkt & Müller (1999) and observed by Rach *et al.* (2014) could have favoured lake level increases by decreased evapotranspiration in the lake catchment.

Phase 3 (12 892–12 820 cal. a BP). – This phase is characterized by high Si:K and low Mn:Fe ratio values. Additionally the flux values for Al and most palynological taxa are distinctly reduced.

The Si:K ratio increases at the beginning of Phase 3 and reflects the recovery of more alkaline conditions in the lake system *c.* 50 years after the LSE. A reorganization of the aquatic life is also indicated by further changes in the sediment record. The stable Mn:Fe ratio and low Al input in this phase, coinciding with lower pollen influx rates of many taxa, are regarded to indicate that no further lake level change occurred. A re-rise in varve thickness and diatom productivity indicates that aquatic bioproductivity returned to a moderate level. The latter is indicated by relatively high TOC:TN ratios. A maximum in spring layer thickness and Si:K ratio that coincides with a Cl accumulation peak and some hypidiomorphic carbonate precipitation between *c.* 12 860–12 840 cal. a BP indicates that this re-increase was driven by intensive circulation of the lake water. That there is no simultaneous peak in the Mn:Fe ratio can be interpreted as an additional indicator of the high lake level inferred for this interval. The reason for the short interruption of varve preservation at *c*. 12 850 cal. a BP remains unclear.

Phase 4 (12 820–12 707 cal. a BP). – The beginning of Phase 4 is characterized by the onset of frequent occurrences of winter layers and a more regular appearance of hypidiomorphic calcite crystals. This is associated with low and decreasing Si:K values, high values of Al and Cl fluxes and generally higher values for most palynological taxa. The Mn:Fe ratio increases distinctly at the beginning of this zone, reaching a maximum at *c.* 12 760 cal. a BP. At the same time accumulation rates for NAP, *Pinus* and *Pediastrum* show maximum values.

These changes indicate that Phase 4 signals another shift in depositional conditions. The decrease in biogenic silica (Si:K), coinciding with higher TOC:TN ratios, points to a decrease in aquatic bioproductivity. The winter layer record indicates a general cooling, whereas the occurrences of autumn diatom blooms and in particular repeated occurrences of hypidiomorphic carbonate precipitation point to turbulent conditions in the summer half of the year. Higher TOC:TN ratios and Cl and Al accumulation is interpreted to reflect stronger westerly winds that resulted in more intensive shore erosion (Baldini *et al.* 2018). The maximum of the Mn:Fe ratio associated with high PARs for most taxa is in line with stronger winds leading to increased bottom water oxygenation. Less pronounced anoxic conditions during a weakened or absent stable summer stratification of the lake water could provide an additional reason for the decreasing Si:K ratio. This would result from the decrease in aquatic bioproductivity and the deeper and more complete mixing due to the onset of stronger winds that led to a limited re-precipitation of biogenic silica during the summer (see Results and interpretation section, varve composition) and a more continuous recycling of biogenic silica. Thus, whereas more intensive mixing possibly fostered diatom spring blooms, the biogenic silica did not find its way into the sediment because of a change in the syn- and postdepositional conditions at the lake bottom. To summarize, the observed sediment record is best explained by the onset of increased wind speeds during the summer half of the year starting at *c.* 12 809 cal. a BP under generally cooling climate conditions at the NAH site.

The return of the influx values of *Betula nana*-type pollen to low pre-LSE influx levels and a simultaneous pronounced minimum of the influx curve of *Betula pubescens*-type pollen at around 12 790 cal. a BP is explained by a local fire event, as reflected in a coinciding maximum of micro-charcoal particles (Krüger *et al.* 2020). This local fire event falls into an interval of Europe-wide repeated fire events that led to the deposition of the so-called Usselo (charcoal) layer especially towards the end of the Allerød period (van Geel *et al.* 1984; van der Hammen & van Geel 2008; Kaiser *et al.* 2009). Often, these soil surfaces are found buried by aeolian redeposition of sands in northern Europe. The assumed increased windiness could partly explain these Allerød period phenomena as it would have induced drier climatic conditions. This could have led to higher frequency of wildfires in particular in coniferous woods, as also assumed for parts of the Early Holocene (Dreibrodt *et al.* 2010; Crombé 2016). The windy conditions would have favoured a return to aeolian activity in sandy landscapes stripped of woods by the wildfires (e.g. Hilgers 2007).

A southwards shift of westerly winds from the north Atlantic preceding the onset of the YD and subsequent to the LSE has already been proposed for *c.* 200 years after the LSE at Lake Meerfelder Maar (Brauer *et al.* 1999) and *c.* 40 years after the LSE at Lake Kråkenes (Lane *et al.* 2013; Baldini *et al.* 2018).

Regarding the geographical position of the Nahe palaeolake and the detected increase in average storminess 135 years after the LSE, our record provides additional evidence for the southward shift of the westerlies prior to the onset of YD conditions. Whereas the southward movement between Lake Kråkenes (62°N) and the Nahe palaeolake (53.5°N) occurred at an average pace of ~10 km a^{-1}, from the Nahe site towards the Meerfelder Maar (50°N) the pace of shifting lowered to ~6 km a^{-1}. Thus, the present study supports the idea of a time-transgressive shift of the north Atlantic climate system, similar to the observations by Lane *et al.* (2013). Since the applied indicators in the studied lakes all imply an abrupt shift towards windier conditions, this change might reflect a long-term response to the LSE, as proposed by Baldini *et al.* (2018).

The results of the high-resolution reconstruction of limnological responses to the LSE from the NAH palaeolake sequence presented here add to arguments for a link between the LSE and the onset of the YD as suggested by Baldini *et al.* (2018). How this compares with the other hypotheses about the YD onset, such as the meltwater pulse (e.g. Johnson & McClure 1976; Berger 1990; Alley 2000; Broecker *et al.* 2010; Schenk *et al.* 2018) or the bolide-impact hypothesis (e.g. Firestone *et al.* 2007; Kennett *et al.* 2009), remains a matter of ongoing research.

Conclusions

The multi-proxy investigation of the annually laminated sediment record from the palaeolake Nahe, northern Germany, allowed the identification of local limnological and environmental changes during the Allerød and in particular responses to the Laacher See eruption (LSE) as follows.

- Little variability characterizes the varve microfacies and geochemical composition prior to the LSE. With respect to the Gerzensee oscillation a weak signal, potentially indicating cooler and windier conditions, has been recorded at the site.
- Regarding the LSE, direct short-term local and probably long-term regional climatic responses can be inferred from the sediment record.
- A serious disturbance of the local environment immediately after the LSE (4 years) resulted from erosion at the shore or in the lake catchment area due to increased storminess and perhaps including heavy precipitation events.
- An acidification of the lake system, probably due to acidic aerosols that originated from the eruption, lasted for about 50 years (12 944–12 890 cal. a BP), a period during which biogenic silica deposition (diatoms) declined and then recovered.
- A lake-level increase between 12 930 and 12 878 cal. a BP is inferred, probably resulting from a change of the water balance as a response to cooling.
- 120 years after the LSE (12 830 cal. a BP) the onset of strong westerly winds is reconstructed and is considered to reflect long-term regional response to the LSE. This intensification of westerly winds has been determined to occur at an earlier stage in Norway (40 years after the LSE) and at a later stage in southwest Germany (200 years after the LSE). The observed delay probably reflects a latitudinal, time-transgressive response of the north Atlantic climate system to the LSE as has been proposed recently.
- A comparison of the timing between the sites implies a changing pace of the southward shift of the westerlies subsequent to the LSE: 40–120 years after the LSE (62°N to 53.5°N) ~10 km a^{-1}, 120–200 years (53.5°N to 50°N) ~6 km a^{-1}.

Acknowledgements. – We are grateful to the landowners that allowed the fieldwork, to Tobias Burau and Sonja Grimm for supporting the fieldwork, and to Manfred Beckers, Imke Meyer and Carola Floors, who helped with laboratory analysis. We would like to thank three anonymous reviewers for their helpful comments. Funded by the Deutsche Forschungsgemeinschaft (DFG, German Research Foundation - Projektnummer 2901391021 – SFB 1266). Open access funding enabled and organized by Projekt DEAL.

Author contributions. – SD did the varve microfacies analysis, geochemical analyses, interpretation, and artwork; SK did the fieldwork, pollen analysis, interpretation, and artwork; JW did the fieldwork and data interpretation; IF did the age depth modelling (OxCal), interpretation, and artwork; all co-authors contributed to manuscript write-up.

References

Alley, R. B. 2000: The Younger Dryas cold interval as viewed from central Greenland. *Quaternary Science Reviews 19*, 213–226.

Baales, M., Joris, O., Street, M., Bittmann, F., Weninger, B. & Wiethold, J. 2002: Impact of the late glacial eruption of the Laacher See volcano, Central Rhineland, Germany. *Quaternary Research 58*, 273–288.

Baier, J., Lücke, A., Negendank, J. F. W., Schleser, G.-H. & Zolitschka, B. 2004: Diatom and geochemical evidence of mid- to late Holocene climatic changes at Lake Holzmaar, West-Eifel (Germany). *Quaternary International 113*, 81–96.

Baldini, J. U. L., Brown, R. J. & Mawdsley, N. 2018: Evaluating the link between the sulfur-rich Laacher See volcanic eruption and the Younger Dryas climate anomaly. *Climate of the Past 14*, 969–990.

Battarbee, R. W., Charles, D. F., Dixit, S. S. & Renberg, I. 1999: Diatoms as indicators of surface water acidity. *In* Stoermer, E. F. & Smol, J. P. (eds.): *The Diatoms: Applications for the Environmental and Earth Sciences*, 85–127. Cambridge University Press, Cambridge.

Battarbee, R. W., Thrush, B. A., Clymo, R. S., Le Cren, E. D., Goldsmith, P., Mellanby, K., Bradshaw, A. D., Chester, P. F., Howells, G. D., Kerr, A., Beament, J. W. L., Holdgate, M. W. & Sugden, T. M. 1984: Diatom analysis and the acidification of lakes.

Philosophical Transactions of the Royal Society of London B, Biological Sciences 305, 451–477.
Berger, W. H. 1990: The Younger Dryas cold spell- a quest for causes. *Global and Planetary Change 89*, 219–237.
Beug, H.-J. 2004: *Leitfaden der Pollenbestimmung für Mitteleuropa und angrenzende Gebiete*. 542 pp. Pfeil, Munich.
van den Bogaard, P. 1995: $^{40}Ar/^{39}Ar$ ages of sanidine phenocrysts from Laacher See tephra (12,900 yr BP): chronostratigraphic and petrological significance. *Earth Planet Science Letters 133*, 163–174.
van den Bogaard, P. & Schmincke, H.-U. 1985: Laacher See Tephra: a widespread isochronous late Quaternary tephra layer in Central and Northern Europe. *Geological Society of America Bulletin 96*, 1554–1571.
Brauer, A. 2004: Annually laminated lacustrine sediments and their palaeoclimatic relevance. *In* Fischer, H., Kumke, T., Lohmann, G., Miller, H. & Negendank, J. F. W. (eds.): *The Climate in Historical Times. Towards a Synthesis of Holocene Proxy Data and Climate Models*, 109–127. Springer, Berlin.
Brauer, A., Endres, C., Günter, C., Litt, T., Stebich, M. & Negendank, J. F. W. 1999: High resolution sediment and vegetation responses to Younger Dryas climate change in varved lake sediments from Meerfelder Maar, Germany. *Quaternary Science Reviews 18*, 321–329.
Brauer, A., Haug, G. H., Dulski, P., Sigman, D. M. & Negendank, J. F. W. 2008: An abrupt wind shift in western Europe at the onset of the Younger Dryas cold period. *Nature Geoscience 1*, 520–523.
Brauer, A., Litt, T., Negendank, J. F. W. & Zolitschka, B. 2001: Lateglacial varve chronology and biostratigraphy of lakes Holzmaar and Meerfelder Maar, Germany. *Boreas 30*, 83–88.
Broecker, W. S., Denton, G. H., Edwards, R. L., Cheng, H., Alley, R. B. & Putnam, A. E. 2010: Putting the Younger Dryas cold event into context. *Quaternary Science Reviews 29*, 1078–1081.
Bronk Ramsey, C. 2008: Deposition models for chronological records. *Quaternary Science Reviews 27*, 42–60.
Bronk Ramsey, C. 2009: *Bayesian analysis of radiocarbon dates. Radiocarbon 51*, 337–360.
Bronk Ramsey, C., Albert, P. G., Blockley, S. P. E., Hardiman, M., Housley, R. A., Lane, C. S., Lee, S., Matthews, I. P., Smith, V. C. & Lowe, G. G. 2015: Improved age estimates for key Late Quaternary European tephra horizons in the RESET lattice. *Quaternary Science Reviews 118*, 18–32.
Crombé, P. 2016: Forest fire dynamics during the early and middle Holocene along the southern North Sea basin as shown by charcoal evidence from burnt ant nests. *Vegetation History and Archaeobotany 25*, 311–321.
Czymzik, M., Dreibrodt, S., Feeser, I., Adolphi, F. & Brauer, A. 2016: Mid-Holocene humid periods reconstructed from calcite varves of the Lake Woserin sediment record (north-eastern Germany). *The Holocene 26*, 935–946.
Davis, M. B. 1968: Pollen grains in lake sediments - redeposition caused by seasonal water circulation. *Science 162*, 796–799.
Davis, M. B. 1973: Redeposition of pollen grains in lake sediment. *Limnology and Oceanography 18*, 44–52.
Davis, M. B. & Ford, M. S. J. 1982: Sediment focusing in Mirror Lake, New-Hampshire. *Limnology and Oceanography 27*, 137–150.
De Klerk, P. 2008: Patterns in vegetation and sedimentation during the Weichselian Late-glacial in north-eastern Germany. *Journal of Biogeography 35*, 1308–1322.
De Klerk, P., Janke, W. F., Kühn, P. & Theuerkauf, M. 2008: Environmental impact of the Laacher See eruption at a large distance from the volcano: integrated palaeoecological studies from Vorpommern (NE Germany). *Palaeogeography, Palaeoclimatology, Palaeoecology 270*, 196–214.
Diesing, K. M. 1866: Revision der Prothelminthen. Abtheilung: Mastigophoren. *Sitzungsberichte der Kaiserlichen Akademie der Wissenschaften. Mathematisch-Naturwissenschaftliche Classe. Abt. 1, Mineralogie, Botanik, Zoologie, Anatomie, Geologie und Paläontologie 52*, 287–401.
Dreibrodt, S., Furholt, M., Hofmann, R., Hinz, M. & Cheben, I. 2017: P-ed-XRF-geochemical signatures of a 7300 year old Linear Band Pottery house ditch fill at Vráble-Ve'lké Lehemby, Slovakia - House inhabitation and post-depositional processes. *Quaternary International 438*, 131–143.
Dreibrodt, S., Lomax, J., Nelle, O., Lubos, C., Fischer, P., Mitusov, A., Reiss, S., Radtke, U., Grootes, P. M. & Bork, H.-R. 2010: Are mid Latitude slope deposits sensitive to climatic oscillations? – Implications from an Early Holocene sequence of slope deposits and buried soils from Eastern Germany. *Geomorphology 122*, 351–369.
Engels, S., van Geel, B., Buddelmeijer, N. & Brauer, A. 2015: High-resolution palynological evidence for vegetation response to the Laacher See eruption from the varved record of Meerfelder Maar (Germany) and other central European records. *Review of Palaeobotany and Palynomorphology 221*, 160–170.
Engels, S., Brauer, A., Buddelmeijer, N., Martin-Puertas, C., Rach, O., Sachse, D. & Van Geel, B. 2016: Subdecadal-scale vegetation responses to a previously unknown late-Allerod climate fluctuation and Younger Dryas cooling at Lake Meerfelder (Germany). *Journal of Quaternary Science 31*, 741–752.
Erdtman, G. 1960: The acetolysis method. A revised description. *Svensk Botanisk Tidskrift 39*, p. 4.
Fægri, K. & Iversen, J. 1989: *Textbook of Pollen Analysis*. 328 pp. Wiley, Chichester.
Firestone, R. B., West, A., Kennett, J. P., Becker, L., Bunch, T. E., Revay, Z. S., Schultz, P. H., Belgya, T., Kennett, D. J., Erlandson, J. M., Dickenson, O. J., Goodyear, A. C., Harris, R. S., Howard, G. A., Kloosterman, J. B., Lechler, P., Mayewski, P. A., Montgomery, J., Poreda, R., Darrah, T., Hee, S. S. Q., Smitha, A. R., Stich, A., Topping, W., Wittke, J. H. & Wolbach, W. S. 2007: Evidence for an extraterrestrial impact 12,900 years ago that contributed to the megafaunal extinctions and the Younger Dryas cooling. *Proceedings of the National Academy of Sciences 104*, 16016–16021.
van Geel, B., De Lange, L. & Wiegers, J. 1984: Reconstruction and interpretation of the local vegetational succession of a lateglacial deposit from Usselo (The Netherlands) based on the analysis of micro- and macrofossils. *Acta Botanica Neerlandica 33*, 535–546.
Grattan, J. & Charman, D. J. 1994: Non-climatic factors and the environmental impact of volcanic volatiles: implications of the Laki fissure eruption of AD 1783. *The Holocene 4*, 101–106.
Gruenert, U. & Raeder, U. 2014: Growth responses of the calcite-loricated freshwater phytoflagellate *Phacotus lenticularis* (Chlorophyta) to the $CaCO_3$ saturation state and meteorological changes. *Journal of Plankton Research 36*, 630–640.
van der Hammen, T. & van Geel, B. 2008: Charcoal soils of the Allerød-Younger Dryas transition were the result of natural fires and not necessarily the effect of an extra-terrestrial impact Netherlands. *Journal of Geoscience - Geologie en Mijnbouw 87*, 359–361.
Hammer, Ø., Harper, D. A. T. & Ryan, P. D. 2001: PAST: paleontological statistics software package for education and data analysis. *Palaeontologia Electronica 4*, http://palaeo-electronica.org/2001_1/past/issue1_01.htm
Harms, E. & Schmincke, H.-U. 2000: Volatile composition of the phonolithic Laacher See magma (12,900 yr BP): implications for the syn-eruptive degassing of S, F, Cl and H_2O. *Contributions to Mineralogy and Petrology 138*, 84–98.
Hilgers, A. 2007: *The chronology of Late Glacial and Holocene dune development in the northern Central European lowland reconstructed by optically stimulated luminescence (OSL) dating*. Ph.D. thesis, University of Köln, 440 pp.
Hogsden, K. L., Xenopoulos, M. A. & Rusak, J. A. 2009: Asymmetrical food web responses in trophic-level richness, biomass, and function following lake acidification. *Aquatic Ecology 43*, 591–606.
Johnson, R. G. & McClure, B. T. 1976: Model for Northern Hemispherical continental ice sheet variation. *Quaternary Research 6*, 325–353.
Kaiser, K., Hilgers, A., Schlaak, N., Jankowski, M., Kühn, P., Bussemer, S. & Przegietka, K. 2009: Palaeopedological marker horizons in northern central Europe: characteristics of Lateglacial Usselo and Finow soils. *Boreas 38*, 591–609.
Kelts, K. & Hsü, J. J. 1978: Freshwater carbonate sedimentation. *In* Lerman, A. (ed.): *Lakes. Chemistry, Geology, Physics*, 296–323, Springer Verlag, Berlin.
Kennett, D. J., Kennett, J. P., West, A., Mercer, C., Hee, S. S. Q., Bement, L., Bunch, T. E., Sellers, M. & Wolbach, W. S. 2009: Nanodiamonds in the Younger Dryas Boundary Sediment Layer. *Science 323*, p. 94.

Kerr, R. A. 2000: A North Atlantic climate pacemaker of the centuries. *Science 288*, 1984–1985.

Krüger, S. & van den Bogaard, C. 2020: Small shards and long distances – three cryptotephra layers from the Nahe palaeolake including the first discovery of Laacher See Tephra in Schleswig-Holstein (Germany). *PaleoRxiv*. https://doi.org/10.31233/osf.io/hzcy3

Krüger, S., Mortensen, M. F. & Dörfler, W. 2020: Sequence completed – palynological investigations on Lateglacial/Early Holocene environmental changes recorded in sequentially laminated lacustrine sediments of the Nahe palaeolake in Schleswig-Holstein, Germany. *PaleoRxiv.* https://doi.org/10.31233/osf.io/bt9m8

Kylander, M. E., Ampel, L., Wohlfarth, B. & Veres, D. 2011: High-resolution X-ray fluorescence core scanning analysis of Les Echets (France) sedimentary sequence: new insights from chemical proxies. *Journal of Quaternary Science 26*, 109–117.

Lane, C. S., Brauer, A., Blockley, S. P. E. & Dulski, P. 2013: Volcanic ash reveals time-transgressive abrupt climate change during the Younger Dryas. *Geology 41*, 1251–1254.

Lange, E., Jeschke, L. & Knapp, D. 1986: *Ralswiek und Rügen. Landschaftsentwicklung und Siedlungsgeschichte der Ostseeinsel. Teil I: Die Landschaftsgeschichte der Insel Rügen seit dem Spätglazial*. 174 pp. Akademie Verlag, Berlin.

Litt, T., Behre, K.-E., Meyer, K.-D., Stephan, H.-J. & Wansa, S. 2007: Stratigraphische Begriffe für das Quartär des norddeutschen Vereisungsgebietes. *Eiszeitalter und Gegenwart 56*, 7–65.

Lotter, A. F. & Birks, H. J. B. 1993: The impact of the Laacher See Tephra on terrestrial and aquatic ecosystems in the Black Forest, Southern Germany. *Journal of Quaternary Science 8*, 263–276.

Lowe, J. J., Rasmussen, S. O., Björck, S., Hoek, W. Z., Steffensen, J. P., Walker, M. J. C., Yu, Z. C. & the INTIMATE group 2008: Synchronisation of palaeoenvironmental events in the North Atlantic region during the Last Termination: a revised protocol recommended by the INTIMATE group. *Quaternary Science Reviews 27*, 6–17.

Merkt, J. 1971: Zuverlässige Auszählung von Jahresschichten in Seesediment mit Hilfe von Groß-Dünnschliffen. *Archiv für Hydrobiologie 69*, 145–154.

Merkt, J. & Müller, H. 1999: Varve chronology and palynology of the Lateglacial in Northwest Germany from lacustrine sediments of Hämelsee in Lower Saxony. *Quaternary International 61*, 41–59.

Meyers, P. A. 1994: Preservation of elemental and isotopic source identification of sedimentary organic matter. *Chemical Geology (Isotope Geoscience Section) 114*, 289–302.

Meyers, P. A. & Ishiwatari, R. 1995: Organic matter accumulation records in lake sediments. *In* Lerman, A., Imboden, D. M. & Gat, J. R. (eds.): *Lakes. Chemistry, Geology, Physics*, 279–328. Springer, Berlin.

Mingram, J., Negendank, J. F. W., Brauer, A., Berger, D., Hendrich, A., Köhler, M. & Usinger, H. 2007: Long cores from small lakes – Recovering up to 100 m-long lake sediment sequences with a high-precision rod-operated piston corer (Usinger-corer). *Journal of Palaeolimnology 37*, 517–528.

Naeher, S., Gilli, A., North, R. P., Hamann, Y. & Schubert, C. J. 2013: Tracing bottom water oxygenation with sedimentary Mn/Fe ratios in Lake Zurich, Switzerland. *Chemical Geology 352*, 125–133.

Newberry, T. L. & Schelske, C. L. 1986: Biogenic silica record in the sediments of Little Round Lake, Ontario. *Hydrobiologia 143*, 293–300.

Peristykh, A. N. & Damon, P. E. 2003: Persistence of the Gleissberg 88-year solar cycle over the last ∼12,000 years: evidence from cosmogenic isotopes. *Journal of Geophysical Research 108*, 1003, https://doi.org/10.1029/2002ja009390.

Peterss, K., Ratzke, U. & Strahl, J. 2002: Geologie von zwei Söllen bei Rosenow, Landkreis Demmin. *In* Kaiser, K. (ed.): *Die jungquartäre Fluß- und Seegenese in Nordostdeutschland. Beiträge zur Tagung in Hohenzieritz (Meckl.) vom 26.-28. Februar 2002*, 22–35. *Greifswalder Geographische Arbeiten 26.*

Prasad, S., Brauer, A., Rein, B. & Negendank, J.F.W. 2007: Rapid climate change during the early Holocene in Western Europe and Greenland. *The Holocene 16*, 153–158.

Rach, O., Brauer, A., Wilkes, H. & Sachse, D. 2014: Delayed hydrological response to Greenland cooling at the onset of the Younger Dryas in western Europe. *Nature Geoscience 7*, 109–112.

von Raden, U. J., Colombaroli, D., Gilli, A., Schander, J., Bernasconi, S. M., van Leeuwen, J., Leuenberger, M. & Eichler, U. 2013: High-resolution late-glacial chronology for the Gerzensee lake record (Switzerland): δ18O correlation between a Gerzensee-stack and NGRIP. *Palaeogeography, Palaeoclimatology, Palaeoecology 391*, 13–24.

Reimer, P. J., Bard, E., Bayliss, A., Beck, J. W., Blackwell, P. G., Bronk Ramsey, C., Buck, C. E., Cheng, H., Edwards, R. L., Friedrich, M., Grootes, P. M., Guilderson, T. P., Haflidason, H., Hajdas, I., Hatté, C., Heaton, T. J., Hoffmann, D. L., Hogg, A. G., Hughen, K. A., Kaiser, K. F., Kromer, B., Manning, S. W., Niu, M., Reimer, R. W., Richards, D. A., Scott, E. M., Southon, J. R., Staff, R. A., Turney, C. S. M. & van der Plicht, J. 2013: IntCal13 and Marine13 radiocarbon age calibration curves 0–50,000 years cal BP. *Radiocarbon 55*, 1869–1887.

Riede, F. 2014: Changes in mid- and far-field human landscape use following the Laacher See eruption (c. 13,000 BP). *Quaternary International 394*, 37–50.

Schenk, F., Väliranta, M., Muschitiello, F., Tarasov, L., Heikkilä, M., Björck, S., Brandefelt, J., Johansson, A. V., Näslund, J.-O. & Wohlfarth, B. 2018: Warm summers during the Younger Dryas cold reversal. *Nature Communications 9*, 1634, https://doi.org/10.1038/s41467-018-04071-5

Schlegel, I., Koschel, R. & Krienitz, L. 1998: On the occurrence of *Phacotus lenticularis* (Chlorophyta) in lakes of different trophic state. *Hydrobiologica 369/370*, 353–361.

Schlegel, I., Koschel, R. & Krienitz, L. 2000: *Phacotus lenticularis* (Chlorophyta) population dynamics in both nature and culture. *Verhandlungen des Internationalen Vereins Limnologie 27*, 700–703.

Schmincke, H.-U., Park, C. & Harms, E. 1999: Evolution and environmental impacts of the eruption of Laacher See Volcano (Germany) 12,900 a BP. *Quaternary International 61*, 61–72.

Schneider, J. & Gebhardt, U. 1995. Aufschlüsse am Salzstock Lieth in Schleswig-Holstein. *In* Plein, E. M. (ed.): *Stratigraphie von Deutschland I. Norddeutsches Rotliegendbecken - Rotliegend-Monographie Teil II*, 96–97. Courier Forschungsinstitut Senckenberg 183, Frankfurt am Main.

Schulz, M. & Mudelsee, M. 2002: REDFIT: estimating red-noise spectra directly from unevenly spaced paleoclimatic time series. *Computers & Geosciences 28*, 421–426.

Smol, J. P. & Boucherle, M. M. 1985: Postglacial changes in algal and cladocerans assemblages in Little Round Lake, Ontario. *Hydrobiologia 103*, 25–49.

Theuerkauf, M. 2003: Die Vegetation NO-Deutschlands vor und nach dem Ausbruch des Laacher See-Vulkans (12880 cal. BP). *Greifswalder Geographische Arbeiten 29*, 143–189.

Weckström, K., Weckström, J., Yliniemi, L.-M. & Korhola, A. 2010: The ecology of *Pediastrum* (Chlorophyceae) in subarctic lakes and their potential as paleobioindicators. *Journal of Paleolimnology 43*, 61–73.

Wersin, P., Höhener, P., Giovanoli, R. & Stumm, W. 1991: Early diagenesis influences on iron transformations in a freshwater lake sediment. *Chemical Geology 90*, 233–252.

Wild, M. 2017: 18 km northwards – zooarchaeological and technological analysis of the Ahrensburgian Assemblage from Nahe LA11 at Lake Itzstedt (Kr. Segeberg/D). *Archäologisches Korrespondenzblatt 47*, 441–461.

Wulf, S., Ott, F., Slowinski, M., Noryskiewicz, A. M., Dräger, N., Martin-Puertas, C., Czymzik, M., Neugebauer, I., Dulski, P., Bourne, A. J., Blaskiewicsz, M. & Brauer, A. 2013: Tracing the Laacher See Tephra in the varved sediment record of the Trzechekowski palaeolake in central Poland. *Quaternary Science Reviews 76*, 129–139.

Zahrer, J., Dreibrodt, S. & Brauer, A. 2013: Evidence of the North Atlantic Oscillation in varve composition and diatom assemblages from recent, annually laminated sediments of Lake Belau, northern Germany. *Journal of Paleolimnology 50*, 231–244.

Zanon, M., Feeser, I., Dreibrodt, S., Schwark, L., Van Den Bogaard, C. & Dörfler, W. 2019: Sustained volcanic impact and ecosystem disturbance over continental Europe during the Early Holocene. *PaleoRxiv*. https://doi.org/10.31233/osf.io/ycrf3

Supporting Information

Additional Supporting Information may be found in the online version of this article at http://www.boreas.dk.

Fig. S1. REDFIT analysis of the pre-LSE varve thicknesses (478 years, tau- 0.66871, bandwidth- 0.005063, oversample- 2, segments- 3, window- rectangle), green line- indication chi square level of 95%; note the occurrence of cycles of 2–3 and 8 years considered to reflect NAO variability, 54 to 62 years probably reflecting AMO cycles, and 93 years perhaps reflecting sun activity (Gleissberg).

Table S1. Total elemental contents of samples of the varved Allerød sequence from the Nahe palaeolake.

Table S2. Correlation matrix of the total elemental content data from Table 1.